Nanomechanical optical fiber

Zhenggang Lian,* Peter Horak, Xian Feng, Limin Xiao, Ken Frampton, Nicholas White, John A. Tucknott, Harvey Rutt, David N. Payne, Will Stewart, and Wei H. Loh

Optoelectronics Research Centre, University of Southampton, Southampton SO17 1BJ, United Kingdom
z.lian@soton.ac.uk

Abstract: Optical fibers are an excellent transmission medium for light and underpin the infrastructure of the Internet, but generally after fabrication their optical properties cannot be easily modified. Here, we explore the concept of nanomechanical optical fibers where, in addition to the fiber transmission capability, the internal core structure of the fiber can also be controlled through sub-micron mechanical movements. The nanomechanical functionality of such fibers is demonstrated in the form of dual core optical fibers, in which the cores are independently suspended within the fiber. The movement-based optical change is large compared with traditional electro-optical effects and we show that optical switching of light from one core to the other is achieved through moving one core by just 8 nm.

OCIS codes: (060.4005) Microstructured fibers; (200.4880) Optomechanics; (060.2280) Fiber design and fabrication.

References and links

1. H.G. Craighead, "Nanoelectromechanical Systems," Science **290**(5496), 1532-1535 (2000).
2. P.F. Van Kessel, L.J. Hornbeck, R.E. Meier, and M.R. Douglass, "A MEMS-based projection display," Proceedings of the IEEE **86**(8), 1687-1704 (1998).
3. Z. Lian, X. Feng, P. Horak, L. Xiao, Y. Jeong, N. White, K. Frampton, J.A. Tucknott, H.N. Rutt, D.N. Payne, W. Stewart, and W.H. Loh. "Optical fiber with dual cores suspended in air," in *The 37th edition of the European Conference on Optical Communication*, Geneva (2011), paper Mo.2.LeCervin.1.
4. P. Russell, "Photonic crystal fibre," Science **299**(5605), 358-362 (2003).
5. F. Yu, W.J. Wadsworth, and J.C. Knight, "Low loss silica hollow core fibers for 3-4 μm spectral region," Opt. Express **20**(10), 11153-11158 (2012).
6. R. Ramaswami and K.N. Sivarajan, "Routing and wavelength assignment in all-optical networks," Networking, IEEE/ACM Transactions on **3**(5), 489-500 (1995).
7. M. Bayindir, F. Sorin, A.F. Abouraddy, J. Viens, S.D. Hart, J.D. Joannopoulos, and Y. Fink, "Metal-insulator-semiconductor optoelectronic fibres," Nature **431**(7010), 826-829 (2004).
8. D. Marcuse, *Theory of Dielectric Optical Waveguides, 2nd Edition*, (Academic Press, 1991).
9. D.C. Abeysinghe, S. Dasgupta, J.T. Boyd, and H.E. Jackson, "A novel MEMS pressure sensor fabricated on an optical fiber," IEEE Photon. Technol. Lett. **13**(9), 993-995 (2001).
10. L. Tong, R.R. Gattass, J.B. Ashcom, S. He, J. Lou, M. Shen, I. Maxwell, and E. Mazur, "Subwavelength-diameter silica wires for low-loss optical wave guiding," Nature **426**(6968), 816-819 (2003).
11. A. Butsch, C. Conti, F. Biancalana, and P.S.J. Russell, "Optomechanical Self-Channeling of Light in a Suspended Planar Dual-Nanoweb Waveguide," Phys. Rev. Lett. **108**(9), 093903 (2012).
12. P. Roberts, F. Couny, H. Sabert, B. Mangan, D. Williams, L. Farr, M. Mason, A. Tomlinson, T. Birks, J. Knight, and P. St. J. Russell, "Ultimate low loss of hollow-core photonic crystal fibres," Opt. Express **13**, 236-244 (2005).
13. V.R. Almeida, Q. Xu, C.A. Barrios, and M. Lipson, "Guiding and confining light in void nanostructure," Opt. Lett. **29**, 1209-1211 (2004).
14. M.J. Weber, *Handbook of Optical Materials*, (CRC Press, Boca Raton, Florida, 2003).
15. K. Van Acoleyen, J. Roels, P. Mechet, T. Claes, D. Van Thourhout, and R. Baets, "Ultracompact phase modulator based on a cascade of NEMS-operated slot waveguides fabricated in silicon-on-insulator," IEEE Photonics Journal **4**(3), 779-788 (2012).
16. F. Xia, L. Sekaric, and Y. Vlasov, "Ultracompact optical buffers on a silicon chip," Nat. Photon. **1**(1), 65-71 (2007).
17. M.L. Povinelli, M. Loncar, M. Ibanescu, E.J. Smythe, S.G. Johnson, F. Capasso, and J.D. Joannopoulos, "Evanescent-wave bonding between optical waveguides," Opt. Lett. **30**, 3042-3044 (2005).

18. I. De Vlaminck, J. Roels, D. Taillaert, D. Van Thourhout, R. Baets, L. Lagae, and G. Borghs, "Detection of nanomechanical motion by evanescent light wave coupling," Appl. Phys. Lett. **90**(23), 233116-3 (2007).
19. T.J. Kippenberg, H. Rokhsari, T. Carmon, A. Scherer, and K.J. Vahala, "Analysis of Radiation-Pressure Induced Mechanical Oscillation of an Optical Microcavity," Phys. Rev. Lett. **95**(3), 033901 (2005).
20. M. Eichenfield, C.P. Michael, R. Perahia, and O. Painter, "Actuation of micro-optomechanical systems via cavity-enhanced optical dipole forces," Nat. Photon. **1**(7), 416-422 (2007).
21. P. Horak, W. Stewart, and W.H. Loh, "Continuously tunable optical buffer with a dual silicon waveguide design," Opt. Express **19**(13), 12345-12461 (2011).

1. Introduction

The harnessing of mechanical interaction in suitably small structures is well-known in silicon MEMS (microelectromechanical systems) and NEMS (nanoelectromechanical systems) devices [1], and these have achieved considerable impact in a wide range of applications, e.g. as accelerometers and gyroscopes, and in 2-D optical switching [2] for displays and reconfigurable optical add-drop multiplexers. Based on our recent realization of a dual suspended core optical fiber [3], we now demonstrate the extension of a MEMS-type functionality to the fiber platform with potentially far reaching applications in, e.g., sensing and optical telecommunications.

The standard optical fiber with its basic core and cladding glass structure has been the workhorse for optical transmission for decades. In recent years, increasingly complex optical fiber designs involving a microstructured cladding and/or core have been suggested [4], and corresponding advances in fabrication techniques made in order to realize them. However, these fiber structures are primarily still targeted at the optical transmission capabilities of the fiber, e.g. to better control its dispersion profile or mode area, or reduce transmission losses over specific wavelength regions [5]. They are also mechanically quite rigid. Apart from the transmission of light, optical networks and systems today incur a considerable amount of processing, such as switching, routing, and buffering of information. Much of this is currently done before or after the fiber, and predominantly in the electronic domain. The incorporation of some of these processing functions into the optical fiber would be advantageous, potentially leading not just to all-optical networks [6], but an integrated "all-fiber" network. We note that optoelectronic fibers that can incorporate light detection in the fiber itself have been reported [7].

We report here the fabrication and demonstration of a nanomechanical optical fiber, where the core of the fiber does not just simply transmit light, but is also capable of controlled nanometer-scale mechanical movements. We have fabricated fibers with two movable cores that are close enough to each other to be optically coupled [3] so that they act as a directional coupler [8]. As a proof of concept of the nanomechanical optical functionality, we demonstrate optical switching of the light through nanometer-scale movement of one of the cores and the subsequent change of the optical coupling length. Conversely, such fibers can be used to detect very small changes in the environment, e.g. pressure or vibration, which will have broad appeal to the field of sensing [9]. Sub-micron diameter optical fibers have previously been fabricated by direct drawing [10] to yield stand-alone single core fibers. While attractive for their evanescent field properties, post-fabrication assembly is required for more complex multi-fiber configurations. The work here demonstrates that low-loss sub-micron optical fibers can be directly fabricated on a draw tower with a conventional 125 μm glass cladding for protection, while containing multiple fiber cores inside the cladding for optical and mechanical interaction.

With such nanomechanical optical fibers we can leverage the manufacturing advantage of optical fibers, where long device lengths – from hundreds of meters to kilometers - are readily fabricated by drawing from a fiber draw tower, with low optical transmission losses. Device lengths can therefore be achieved that are much greater than is possible on a silicon MEMS chip, and the sensitivity of these fiber-based devices to motion or changes in the environment can be correspondingly greater. Our results show that such fibers are capable of responding

optically to nanometer movements in the fiber cores. The sensitivity to nanometer displacements of a dual slab fiber structure has also recently been analyzed theoretically [11].

2. Fabrication and experimental results

The dual core fibers (Fig. 1 (a) shows a schematic graph of the fiber concept) were fabricated using lead silicate glasses. Lead silicate glasses were chosen because of their lower melting points, which enable the glass extrusion technique to be adapted to produce the desired dual core preform structure (although the drawn fiber cross-section differs systematically from that of the preform). Figure 1(b) shows a centimeter-scale extruded glass preform corresponding to the conceptual structure.

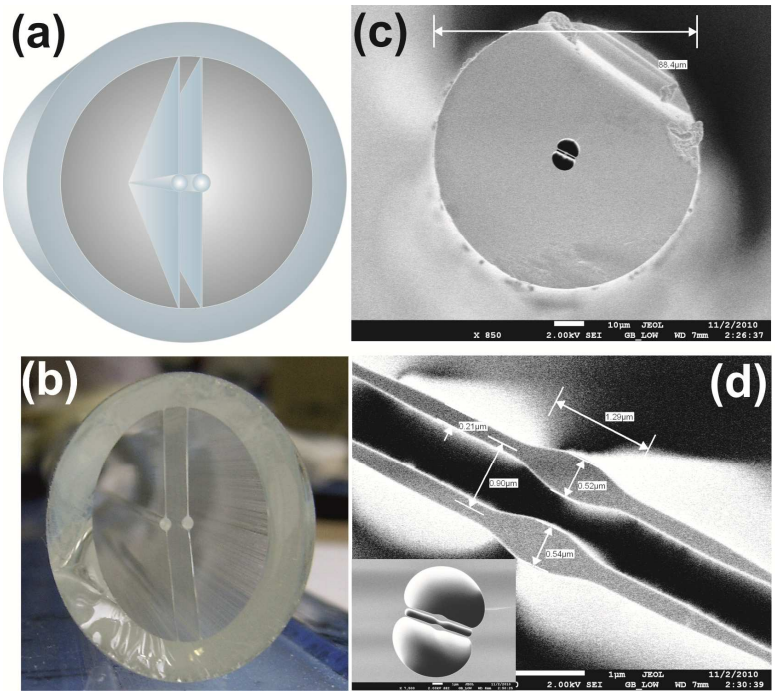

Fig. 1. (a) Schematic of the dual core nanomechanical optical fiber concept. (b) Extruded glass preform of the desired structure. (c) SEM photograph of a fabricated dual suspended core optical fiber; and (d) magnifies of the core structure.

For the extrusion, a glass billet was placed inside an extrusion die and heat applied to raise the temperature until the glass reached its softening point. The glass was then extruded through a custom-designed stainless steel die to form the central portion of the fiber preform. The extrusion die has two slots each with a circular hole in the middle of the slot that on extrusion produces the two cores in the preform as shown in Fig. 1(b). The slots were initially designed to be parallel to directly produce straight glass membranes upon extrusion; however, it proved difficult to extrude the glass through the die with two parallel slots very close together, due to the high load (nearly half a ton at the softening temperature of the glass) needed to be applied to the glass during this extrusion process. The slots were therefore made curved away from each other, to increase the space between the cores; however, during the fiber drawing process, the curved glass membranes straighten up due to surface tension forces, resulting in straight glass membranes for the fiber. For Schott F2 glass, the extrusion furnace temperature was 590ºC, and the extrusion was conducted at a constant speed; the extrusion

rate through the die was 0.052 mm per minute (taking 9 hours to extrude the 30 mm length glass billet). The slow extrusion speed was necessary to enable the glass to flow properly through the narrow channels of the die, in order to minimize die swell and preform distortion. The extruded preform has an outer diameter of 16 mm.

The preform was placed on a fiber draw tower and caned down to 1 mm in diameter. The dual core cane was then placed inside a Schott F2 glass jacket tube (used as the cladding for the dual core fiber), and finally drawn into the desired fiber, at a temperature of 730 ºC. The relatively low fiber drawing temperature was chosen to prevent the fiber cores from distorting (elongating) further.

The dual movable core fiber fabricated using lead silicate glass is shown in Fig. 1(c) and (d). Although the cores are circular in the glass preform, they are elongated during fiber drawing. This is due to surface tension forces which become very substantial at these small dimensions, and careful control of the drawing conditions during the fiber draw process is required. The sub-micron sized cores and core separation dimensions are chosen so that the two cores will be optically coupled through their evanescent fields. Each core is held suspended in air from the outer glass cladding by two glass membranes which are ~200 nm thick, so that the cores can move freely in the direction perpendicular to the membranes.

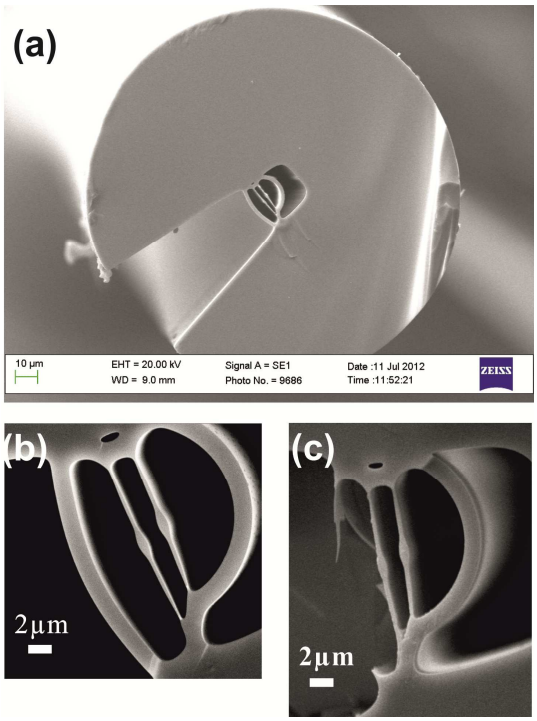

Fig. 2. SEM photographs of a dual core fiber with a direct access channel to one of the cores for pressure actuation. (a) Fiber structure after drawing. (b) Close-up of the fiber core structure. The displacement between the two cores is 2 µm. Cores are 0.8 µm ×2.7 µm in size. (c) Fiber core structure after the remaining wall of the cladding has been etched away.

For direct verification of the nanomechanical optical functionality of these fibers we fabricated an additional channel through the fiber cladding that provides direct fluid access to the environment from the open hole adjacent to one core, by etching through a portion of the cladding wall.

For creating an access channel to the core, the F2 glass jacket tube (used as the cladding in the preform) was first modified by having a 0.95 mm wide slot cut vertically from the surface at one side of the tube through to the center. The dual core cane was placed inside this

slotted tube to form the fiber preform, and drawn into fiber (Fig. 2 (a) and (b)). To remove the remaining thin glass wall separating the core from the outside environment, a buffered hydrofluoric acid etch was applied. The etch rate for the thin glass wall is 0.25±0.01 µm /min, to yield the final fiber structure shown in Fig. 2(c). Creating this access channel allows us to apply direct pressure selectively to one core, and move it in a controlled manner to achieve optical switching. The optical propagation losses of the fiber were experimentally determined using the fiber cut-back method; the results are displayed in Fig. 3.

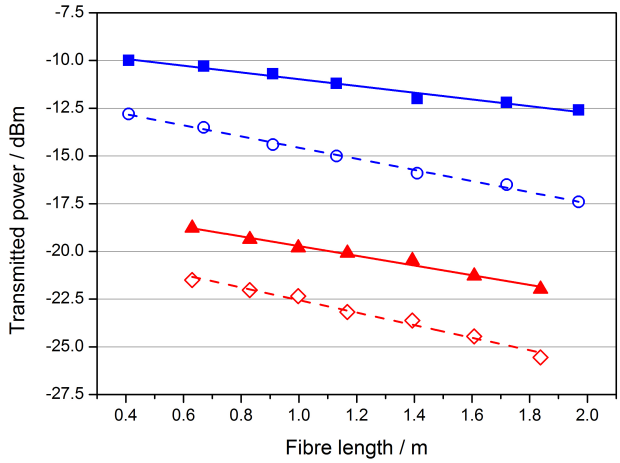

Fig. 3. Optical propagation loss measurements of the dual core fiber in Fig. 2, using the fiber cut-back measurement method. The losses for both horizontal (TE) and vertical (TM) polarization modes, and at two different wavelengths (1550nm and 1047nm) were measured. Cut back data point: ■ 1047 nm, TE; ○ 1047 nm, TM; ▲ 1550 nm, TE; ◊ 1550 nm, TM. Curve fittings: solid blue: -1.77 dB/m, 1047 nm, TE; dashed blue: -2.92 dB/m, 1047 nm, TM; solid red: -2.54 dB/m, 1550 nm, TE; dashed red: -3.29 dB/m, 1550 nm, TM.

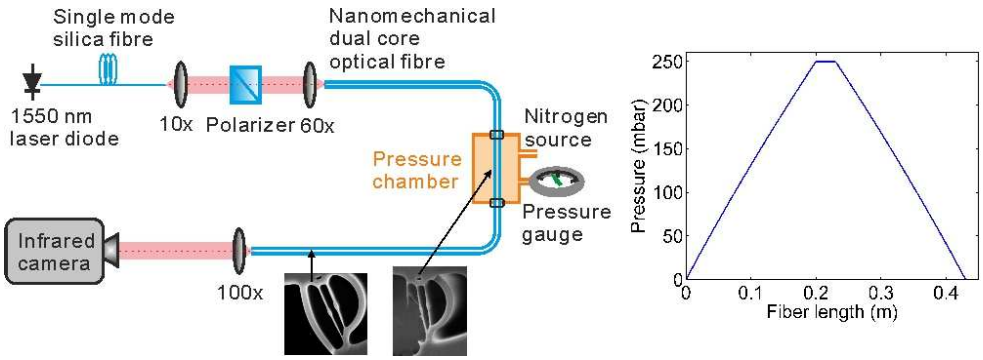

Fig. 4. (Left) Experimental set-up with dual core fiber to show optical switching by pressure actuation on one core. Dual core fiber of length 43 cm used for test. A 3 cm section of the fiber in the middle is etched for direct pressure access to one core. The in-house designed pressure chamber has one pipe connected to a nitrogen gas line and another to a pressure gauge. (Right) Calculated pressure profile inside the pressurized hole of the dual core fiber.

The experimental configuration for demonstrating nanomechanical optical switching in the fiber is shown in Fig. 4 (left). The fiber length was 43 cm, with a 3 cm section in the middle of the fiber etched through to gain direct access to one core. The etched part of the fiber was placed in an in-house constructed pressure chamber. Light from a 1550 nm wavelength pigtailed laser diode (2mW) was collimated, sent through a polarizer, and focused using a 60x objective into one of the fiber cores. The polarization state of the light was parallel to the long elliptical axis of the core; we select this polarization state as it yields a lower optical propagation loss (2.54 dB/m) than with the orthogonally polarized state (3.29 dB/m). For the 0.4m length of fiber used, the fiber loss is therefore ~ 1dB.

The light output from the dual core fiber was imaged via a 100x objective onto a near-infrared video camera (Electrophysics MicronViewer 7290A), and monitored in real time. Figure 5 (top, (a) to (k)) shows the change in the light intensity pattern observed on the IR video camera as the pressure in the chamber is increased. The optical intensity shifts from one core to the other and back again as the pressure continually increases, exhibiting an optical response that is periodic with pressure (Fig. 5 (bottom)). Such a sinusoidal behavior is in fact expected from coupled mode theory: For the small core displacements observed in our fiber (a few nanometer, as discussed below), the displacement depends linearly on the applied pressure, which in turn leads to a linear change of the optical core-to-core coupling. The resulting change of the modal beat length thus leads to periodic switching with pressure over a fixed fiber length. The periodicity can be seen most clearly from the plot, where the horizontal axis is the applied pressure in mbar and the vertical axis is the normalized optical output, defined as the power from one core divided by the sum of the power from both cores. The pressure period (for the light to switch from one core to the other and back again) is approximately 100 mbar. A maximum 248 mbar was applied to the fiber, spanning 2.5 periods. This switching behavior is readily repeatable; by ramping the pressure up and down, the same optical intensity pattern was observed for a given pressure.

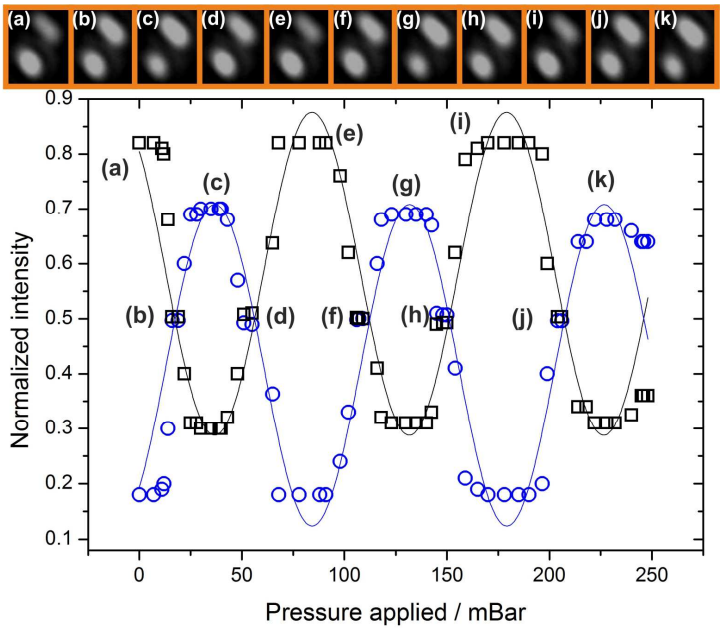

Fig. 5. (Top) Optical intensity observed on the infrared video camera for different applied pressures. (Bottom) Plot of intensity in one core as a function of applied pressure, showing the periodic switching behavior. ○ Hollow circle: normalized intensity of the upper core; □ hollow square: normalized intensity of the lower core; solid line (blue): curve fitting to the upper core; solid line (black): curve fitting to the lower core.

3. Analysis

The experimental data connecting the optical behavior of the fiber to the applied pressure allows us to determine the amount of movement that was imparted to the fiber core for optical switching. The mechanical and optical behavior of the suspended cores can be modeled knowing the refractive index (1.6 at wavelength of 1550 nm) and Young's modulus (57 GPa) for the lead silicate (Schott F2) glass that the fiber was made from. The physical dimensions of the fiber cores and the glass membranes suspending them were obtained from SEM photos (Figs. 2 and 6 (left)), and the optical modes supported by the fiber are numerically calculated using a full vectorial Finite Element Method (Comsol Multiphysics®).

At these dimensions, each core of the fiber is multimoded, with two low loss TE (horizontal polarization) modes and two TM (vertical polarization) modes; the optical intensity distributions calculated for these modes are shown in Fig. 6 (right). Single mode operation will require reducing the core ellipticity to achieve smaller core dimensions; this is a challenging problem for the fabrication process and a subject of continuing investigation. The optical switching behavior can be viewed as an interference effect of light propagating in the "supermodes" of the compound dual-core fiber structure, which consist of quasi-even and quasi-odd superpositions of the individual core modes [8]. We note that TE mode operation as well as TM mode operation is possible, with the latter showing larger losses as discussed above but generally slightly stronger core-to-core coupling.

The simulations also showed that the corresponding modes of the two cores have slightly different propagation constants (effective index difference ~$3x10^{-4}$ for the fundamental modes), probably due to the distortion of the fiber geometry by the introduction of the additional channel required for the pressure-switching experiment. This phase mismatch between the cores prevents perfect optical coupling and is currently the limiting factor to the extinction ratio shown in Fig. 5 of 8 dB.

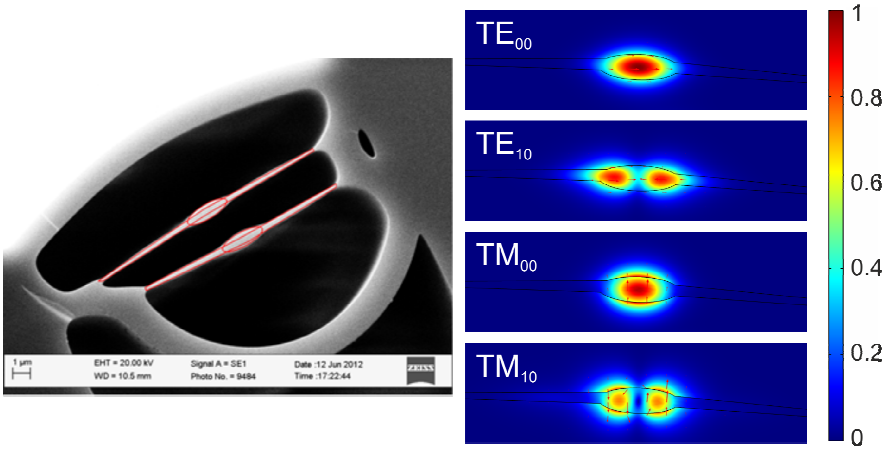

Fig. 6. (Left) The red curves in the SEM photo denote the geometry used in the modeling calculations. (Right) Calculated TE (horizontal polarization) and TM (vertical polarization) modes of a single core in the dual core fiber (normalized to the maximum of the TE_{00} mode).

The wavelength and polarization dependent fiber propagation losses $\alpha_{fiber}(\lambda)$ for these modes can be estimated by considering the net loss as the sum of the bulk glass loss and surface optical scattering:

$$\alpha_{fiber}(\lambda) = \alpha_{glass}(\lambda) + \alpha_{surface}(\lambda) \qquad (1)$$

For the lead silicate glass used, the bulk material loss $\alpha_{glass}(\lambda)$ is relatively high: 1.75 dB/m at 1550nm and 0.35 dB/m at 1 micron (Schott F2 glass data sheet). The surface optical scattering

loss $\alpha_{surface}(\lambda)$ can be estimated using the *F*-factor quantifying the overlap between the optical mode with the glass surface, normalized to the total power in the mode [12]:

$$\alpha_{surface}(\lambda) \sim F / \lambda^3 \qquad (2)$$

At the wavelength of 1550 nm, the *F*-factor for the fundamental TE and TM modes are 1.58 x 10^6/m and 2.96 x 10^6/m respectively. We note that the surface optical scattering for the TM mode is almost twice that for the TE, because the electric field in the TM mode is stronger at the air interface of the waveguide core [13]. At 1 micron wavelength, the TE and TM modes are more confined within the core, and therefore yield smaller *F*-factors of 0.97 x 10^6/m and 1.7 x 10^6/m, respectively.

The results of the loss calculations are shown in Table 1, and compared with the corresponding cut-back loss measurements of Fig. 3. There is good agreement with the experimentally determined losses. With the use of glasses with lower bulk material losses, transmission losses at 1550 nm should be less than 1 dB/m, and will be limited only by surface scattering.

Table 1. Optical fiber loss comparison between the experimental measurements and the losses calculated from the numerical model.

Wavelength	TE(measured)	*TE(calculated)*	TM(measured)	*TM(calculated)*
1.55 μm	2.54	*2.50*	3.29	*3.15*
1 μm	1.77	*1.84*	2.92	*2.96*

The mechanical response of the fiber to applied pressure was also calculated. From the classical Euler-Bernoulli beam equation, we note that the mechanical motion will be a strong function of the dimensions of the glass membrane structure, scaling as (h^4/d^3E) *p*, where *h* and *d* are the height and thickness of the membrane respectively, *E* the Young's modulus for the glass, and *p* the applied pressure. Accurate numerical modeling using the Finite Element Method and including the elliptical core feature confirms this; more importantly, the calculations show that the fiber core moves by 0.08 nm for each 1 mbar change in pressure applied to it.

For the experimental configuration used in Fig. 4 (left), where both fiber ends are open to the atmosphere, the pressure applied at the center of the fiber decreases approximately linearly with distance to the end of the fiber, as confirmed by a finite element fluid dynamics simulation (Fig. 4, right). Using this pressure profile, the field profile for the first TE optical mode, and the mechanical response of the fiber, the modeling calculations show that optical switching from one core to the other occurs for 98 mbar in applied pressure. This is in reasonable agreement with the experimentally observed value of ~50 mbar. The slightly lower pressure values found experimentally for achieving optical switching may be due to the thin glass membranes being weaker - from surface defects such as micro- or nano-cracks - than was assumed in the calculations, which used the bulk Young's modulus for the glass. 98 mbar of applied pressure corresponds to just 8 nm of movement of the core for this fiber. We note that for this calculation, we have taken into account the change in the refractive index of the nitrogen on one side of the core due to the increase in pressure, equal to 2.8 x 10^{-5} per 100 mbar [14]. Although this change in refractive index of the gas is small, the effect on the optical behavior is not insignificant when compared to the nanometer-level motion of the core, and accounts for ~10% of the optical switching response (i.e. the core would have to move by 7 nm, instead of 8 nm, for optical switching to take place in the absence of the pressure-related index change). On the other hand, the results are rather insensitive to temperature fluctuations, with a shift of the interference fringes by ~0.25% per Kelvin. For the low optical powers used (2mW), we therefore expect the temperature contribution to the observed optical behaviour to be minor at best.

The agreement between the theory and the experimental data provides validation to our concept of the dual core nanomechanical fiber. With our numerical model, we can consider the potential of such fibers. The mechanical resonance frequency of the fiber structure is on the order of 1 – 10 MHz (for already achieved ranges of dimensions, Figs. 1(c), (d) and Fig. 2 (a) to (c)), suggesting that µs switching times are possible. The resonance frequency f can be optimized with the fiber dimensions, scaling with the thickness and height of the glass membranes as $f \sim d/h^2$.

While we have used the application of gas pressure on the core for the initial switching demonstration of this fiber, there are a number of other - faster - actuation mechanisms that can potentially be used, for example, electrostatic actuation which is a common approach in silicon MEMS devices [15]. These nanomechanical optical fibers also offer considerable potential towards realizing functionalities and applications that have proved hard to achieve so far, such as self-configurable or "smart fibers", and optical buffers [16]. It has been previously pointed out that self-optical switching can be accomplished using the optical force from the propagating signal to move the waveguide itself [17]. While the use of optical force switching has been demonstrated in semiconductor waveguides [18] and using microresonators [19, 20], the low propagation losses and long fiber lengths will allow for lower optical powers in reaching the self-switching threshold, opening the way for the development of self-configurable or 'smart' fibers. The fiber presented here was optimized for the switching by pressure and shows negligible optical forces (corresponding to <0.001mbar for 100mW optical power). However, our preliminary simulations suggest that optical-induced pressures up to 0.1 mbar for 100mW of optical power can be achieved by reducing the gap size to 100nm, which would allow for optical switching over fiber lengths of a few meters. Practical applications may require the dual core fiber to be spliced to standard single-mode fiber (SMF). Due to the size mismatch, butt coupling/splicing will only couple the symmetric mode of the dual core fiber into the SMF. Coupling a single core to the SMF could be achieved by an intermediate section of fiber containing a single suspended core, whereas coupling the two cores to separate SMFs (as required for switching) will necessitate a dual-core taper that converts the submicron modes of our fiber to micron dimensions similar to standard fiber couplers.

Apart from switching and sensing applications, the dual core fiber has the further useful property of a continuously variable propagation delay time that can be controlled through adjusting the separation distance between the two cores [21]. Although the fractional change in time delay achievable - about 10% of the total propagation time through the fiber - is relatively small (albeit high by electro-optic standards), the ability to use long fiber lengths can yield substantial net variable time delays (up to a nanosecond or more of variable delay per meter of fiber, with the use of high index glasses), which would make this an attractive candidate for realizing optical fiber buffers.

4. Conclusion

We have described the development of nanomechanical optical fibers, which have been realized initially in the form of dual suspended core fibers. The nanomechanical functionality is shown in an optical switching demonstration through moving one core by just 8 nm. The dual suspended core fibers are highly responsive to nanometer-scale mechanical movements within the fiber, and should open up new possibilities in fiber functionality, including optical sensing applications, as well as smart self-configurable optical fibers and optical buffering.

Acknowledgements

We gratefully acknowledge funding support for this work from the Engineering and Physical Sciences Research Council (EPSRC) via the EPSRC Centre for Innovative Manufacturing in Photonics, and the "Photonic Hyperhighway" Programme Grant.